



# Thiophene-2-carbonitrile: a bifunctional electrolyte additive to improve the performance of lithium-ion batteries

Caishuo Yin<sup>1</sup> · Xianming Wu<sup>1</sup> · Xianwen Wu<sup>1</sup> · Xiuting Wu<sup>1</sup> · Mengfan Zhang<sup>1</sup>

Received: 13 September 2022 / Revised: 22 February 2023 / Accepted: 26 February 2023 / Published online: 11 March 2023  
© The Author(s), under exclusive licence to Springer-Verlag GmbH Germany, part of Springer Nature 2023

## Abstract

Thiophene-2-carbonitrile (CT) is used as an electrolyte additive to improve the cycle performance of Li/LiNi<sub>0.5</sub>Mn<sub>1.5</sub>O<sub>4</sub> (LNMO) cells. The effects of CT on the electrode interface and cycling performance of Li/LNMO cells are studied by electrochemical methods such as charge–discharge measurements, cyclic voltammetry (CV), electrochemical impedance spectroscopy (EIS), scanning electron microscopy (SEM), X-ray photoelectron spectroscopy (XPS), transmission electron microscopy (TEM), and other characterization methods. Results show that CT can be oxidized before the electrolyte, forming a polythiophene protective film on the electrode surface, which improves the interphase stability of the electrode/electrolyte. The Li|1.0 M LiPF<sub>6</sub>-EC/EMC/DMC (1:1:1, v/v/v) |LNMO cell with 0.1 wt% CT shows a capacity retention of 91.2% after 300 cycles at a charge–discharge rate of 1 C between 3.5 and 4.95 V. The addition of thiophene-2-carbonitrile can significantly improve the cycle performance of Li/LiNi<sub>0.5</sub>Mn<sub>1.5</sub>O<sub>4</sub>.

**Keywords** Thiophene-2-carbonitrile · Electrolyte additive · LiNi<sub>0.5</sub>Mn<sub>1.5</sub>O<sub>4</sub> · Lithium-ion batteries

## Introduction

Lithium-ion batteries are gaining huge attention due to their high energy density and long cycle life [1, 2]. However, their energy density is still insufficient for electric vehicles and energy storage applications. A cathode material with high-specific capacity and operating voltage is required to achieve the high energy density of a lithium-ion battery [3–8].

LiNi<sub>0.5</sub>Mn<sub>1.5</sub>O<sub>4</sub> is a promising cathode material and has attracted wide attention for its high operating voltage (4.75 V vs. Li/Li<sup>+</sup>) and high theoretical specific capacity (146.7 mAh g<sup>-1</sup>) [9]. However, the high voltage of LNMO can make traditional organic carbonate-based electrolytes decompose, resulting in harmful side reactions that deteriorate an electrode/electrolyte interface and reduce cycle life. Additionally, the dissolution of transition metal ions during the cycle accelerates the decay of capacity.

To resolve the issue, several methods are used to improve the surface stability of LNMO such as ion doping [10], coating [11], employing high-concentration electrolytes [12],

and selecting functional additives [13]. Among these methods, adding a small number of additives to an electrolyte system can form a beneficial protective layer in situ on an electrode surface and can improve the surface stability of LNMO effectively. The method is easy to use and replacing existing equipment is not required.

Thiophene and its derivatives as functional additives can form a uniform and compact coating on the electrode surface before the decomposition of an electrolyte solvent, which can prevent the decomposition of solvents and salts in an electrolyte. Furthermore, polythiophene generated by electrochemical oxidation generally has excellent chemical stability and high conductivity, which improves the cyclic stability of high-pressure cathodes [14]. Thiophene (TH), 2,2'-bithiophene (2TH) and 2,2'-:5'-,2'-terthiophene (3TH) were used as functional additives to inhibit electrolyte decomposition of LiCoO<sub>2</sub> during high-voltage cycling. In comparison with 1 M LiPF<sub>6</sub>, EC:DMC = 3:7 (Vol%) blank electrolyte and cycled for 100 cycles at the current density of 0.25 C and voltage range 3.0–4.4 V, the capacity retention rate of LiCoO<sub>2</sub> electrodes with 0.1 wt% TH, 2TH, and 3TH increased by 15.3, 27.4, and 34.8%, respectively [15]. A total of 0.25% terthiophene was added to a standard (1 M LiPF<sub>6</sub>, EC:DMC = 1:2 (Vol%)) electrolyte, and the capacity retention of Li/LNMO cells after 350 cycles improved from 50 to 91% [16].

✉ Xianming Wu  
xianmingwu@163.com

<sup>1</sup> College of Chemistry and Chemical Engineering, Jishou University, Jishou 416000, Hunan, China

Some additives with  $-C\equiv N$ , such as succinonitrile [17], fumaronitrile [18], 1,3,6-hexanetricarbonitrile [19], and 1,3,5-pentanetricarbonitrile [20], have been reported and employed as electrolyte additives for high voltage lithium-ion batteries. The additives can contribute to the formation of a conductive and stable SEI layer on an anode. The nitrile group in the additive can preferentially cooperate with the high-valence transition metal atoms on an electrolytic cathode, thereby reducing the parasitic reaction between the delithiated cathode surface and electrolyte [21, 22].

Based on the above consideration, we selected 2-thiophenitrile as a novel high-voltage electrolyte additive for Li/LNMO cells. The effect of electrolyte additives on the electrochemical and physical characteristics of electrodes was studied by linear sweep voltammetry (LSV), CV, SEM, TEM, and XPS.

## Experimental

### Preparation of cells

The base electrolyte (Guangdong Canrd New Energy Technology Co., Ltd., China) consists of 1 M  $LiPF_6$  dissolved in a mixed solvent (ethylene carbonate (EC) to ethyl methyl carbonate (EMC) to dimethyl carbonate (DMC) = (1:1:1 (v/v/v))). Thiophene-2-carbonitrile (purity > 98%) was purchased from Sinopharm Chemical Reagent Co., Ltd. Furthermore, the CT electrolyte was prepared by adding 0.1 and 0.2 wt% CT to the base electrolyte. A cathode slurry consisting of  $LiNi_{0.5}Mn_{1.5}O_4$  (China Xingneng Co., Ltd.), conductive acetylene black, and adhesive polyvinylidene fluoride (PVDF) was mixed in N-methyl-2-pyrrolidone solution based on the mass ratio of 8:1:1 and stirred for 12 h. The slurry was spread evenly on the surface of an aluminum foil and heated at 80 °C for 4 h. The aluminum foil spread with LNMO was finally cut into a disk of 14 mm diameter. The 2032-type coin cells with LNMO as a cathode and lithium sheet as an anode were prepared in an argon-filled glove box with  $H_2O < 0.1$  ppm and  $O_2 < 0.1$  ppm.

### Electrochemical measurements

The electrochemical performance of Li/LNMO and Li/Li cells was determined using a Neware test system at 25 °C. The Li/LNMO cells were cycled in a voltage range of 3.5–4.95 V at 0.2 C for the first 3 cycles and then at 1 C for the subsequent cycles. Additionally, each charge process included a constant voltage (4.95 V) until the cut-off current was 0.1 C. Galvanostatic Li plating/stripping tests of Li//Li cells were conducted at a current density of  $0.5 \text{ mA cm}^{-2}$  with a plating/stripping capacity of  $0.5 \text{ mAh cm}^{-2}$ . Furthermore, CV, linear sweep voltammetry (LSV), and EIS were performed on a Chi660 electrochemical workstation (Shanghai Chenhua Company).

The scan rate of CV for the Li/LNMO cell is set from 3.5 to 4.95 V at a rate of  $0.1 \text{ mV s}^{-1}$ . The LSV of the “V-type” battery is scanned from open-circuit voltage to 6 V with a scanning speed of 1 mV/s using platinum and lithium as working and auxiliary/reference electrodes, respectively. The operating frequency range of Li/LNMO cells EIS was 0.01 to  $10^5$  Hz and the amplitude was 5 mV.

### Surface characterization

The cycled LNMO electrodes and lithium foils were washed with anhydrous DMC three times to remove salt and other residues from the surface of the LNMO electrode and lithium foils. The surfaces of the cycled LNMO cathodes and lithium foils were characterized by SEM technique (TESCAN MIRA LMS). The surface composition of the cycled LNMO cathodes was analyzed by XPS (Thermo Scientific ESCALAB Xi+). Furthermore, TEM (JEOL JEM 2100F) was used to investigate the film image on the LNMO electrodes. The crystal structure was studied by X-ray diffraction (XRD) in the  $2\theta$  range of 10–80°. The oxidation products of electrolytes were verified by the Fourier transform infrared (FTIR, Nicolet I S10). An inductively coupled plasma emission spectrometer was employed to measure the deposition amount of metal ions on lithium anodes (ICP-OES, Avio 200).

## Results and discussion

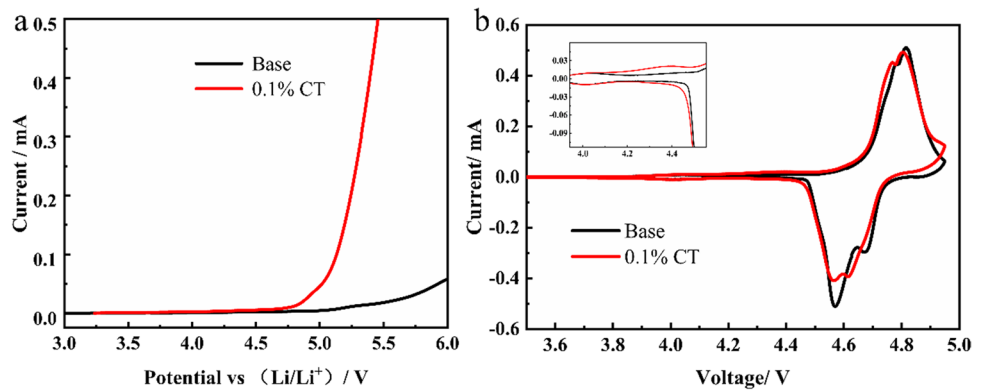
### Oxidation ability of CT

Figure 1 shows a linear scan curve of the electrolyte with and without additive of CT, and it shows that the oxidation current of the electrolyte without additive of CT starts at approximately 5 V. However, for the electrolyte with additive CT, a significant oxidation peak appears at approximately 4.5 V, which indicates its higher oxidation activity and preferential oxidation before electrolyte solvent decomposition. The oxidation of CT can be more clearly visualized via the CV test of Li/LNMO batteries. As shown in Fig. 1b, a small redox peak is observed in the two samples at approximately 4.0 V corresponding to the redox of  $Mn^{3+}/Mn^{4+}$ , while a redox peak between 4.5 and 4.9 V is the redox peak of  $Ni^{4+}/Ni^{2+}$ . However, an additional oxidation peak at approximately 4.4 V appears in the electrolyte with 0.1% CT additive, which is the oxidation signal of CT. The observation is consistent with the results of LSV.

### Electrochemical performance

Figure 2a, b shows the cycle performance and the Coulomb efficiency of Li/LNMO battery using the electrolyte with

**Fig. 1** The LSV (a) and CV (b) curves of the electrolyte with and without CT additive



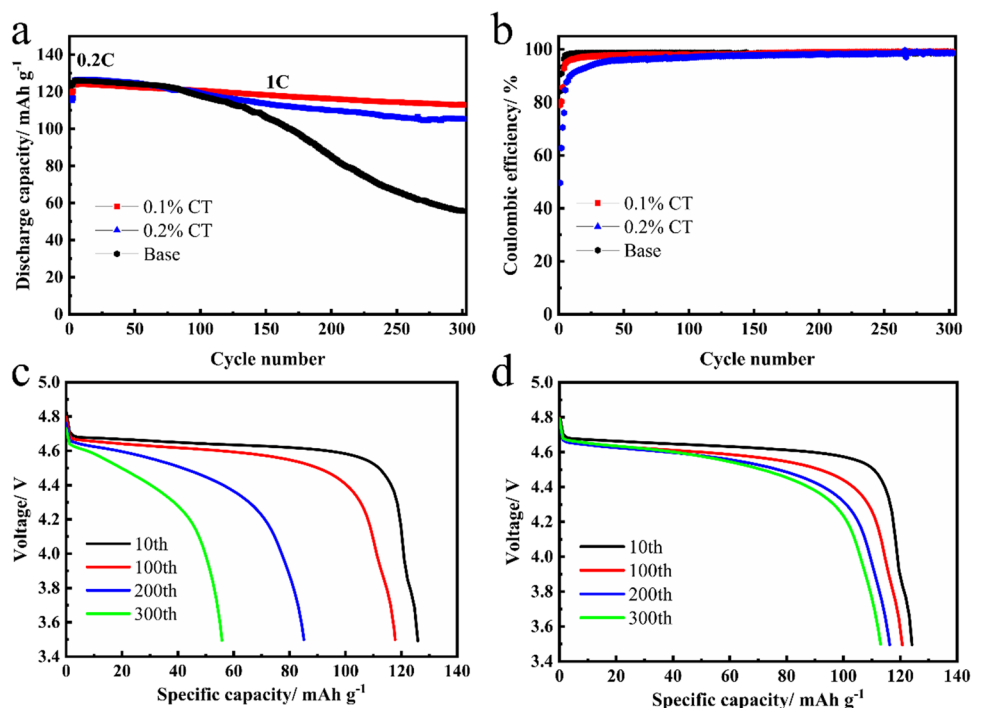
and without CT additive at room temperature. Additionally, the discharge-specific capacity of Li/LNMO battery using the electrolyte without CT additive decreases from 125.83 to 55.60 mAh g<sup>-1</sup> after 300 cycles. The capacity retention rate is only 44.18%. The sharp decline in capacity is caused by the destruction of the electrode structure and decomposition of electrolytes under a high voltage cycle. While for the electrolyte with 0.1% CT, the discharge-specific capacity of the Li/LNMO battery is still 112.94 mAh g<sup>-1</sup>, and the capacity retention rate is 91.2%. However, the Coulomb efficiency and capacity retention decrease CT increases to 0.2%.

Figure 2c, d shows the evolution of charge and discharge profiles of Li/LNMO batteries with different electrolytes. The discharge plateau gradually decreases with the increase in cycle times. This indicates the presence of a severe polarization for the electrolyte without adding CT during cycling.

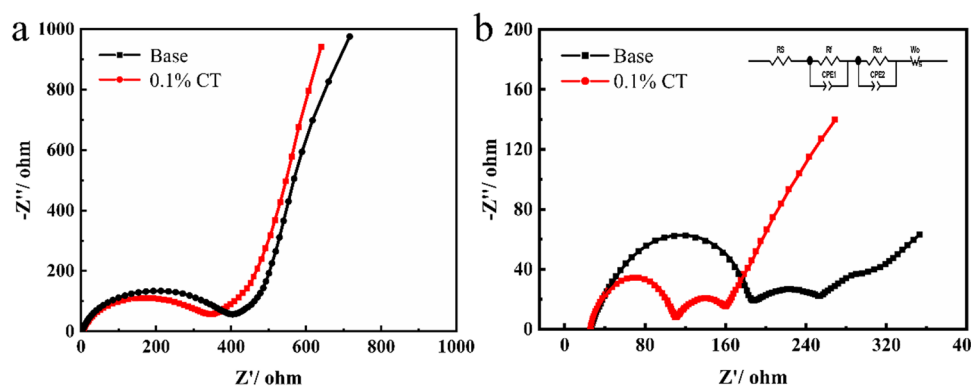
However, the voltage curve for the electrolyte with the addition of 0.1% CT is relatively stable. This may be due to that CT is favorable to forming the protective layer on the electrode, which can inhibit the decomposition of electrolytes effectively.

Figure 3 shows the electrochemical impedance spectra in the electrolyte with and without CT additive after the initial cycle and after 300 cycles in the discharge state at room temperature. The impedance of the two electrolytes consists of three parts. The high-frequency region of the semicircle represents the interface impedance ( $R_f$ ), which is related to the resistance of Li<sup>+</sup> passing through the electrode surface film. The middle-frequency range of the semicircle region represents the charge transfer impedance ( $R_{ct}$ ). A linear line in the low-frequency part is the Weber impedance ( $W_o$ ) [23–25].

**Fig. 2** Cycling stability (a) and the Coulombic efficiency (b) of Li/LNMO cells in the electrolyte with and without CT at room temperature; selected discharge profiles in the electrolyte without additive of CT (c) and in the electrolyte with 0.1% CT additive (d)



**Fig. 3** Electrochemical impedance spectra of cell in the electrolyte with and without additive of CT after the initial (a) and 300 cycles (b)



**Table 1** The resistance of Li/LNMO cells in the electrolyte with and without CT the additive obtained from the Nyquist plots with equivalent circuit model by Zview program

Sample	After the initial cycle		After the 300 cycles	
	$R_f/\Omega$	$R_{ct}/\Omega$	$R_f/\Omega$	$R_{ct}/\Omega$
Base	184.7	208.7	116.3	25.6
0.1% CT	76.6	200.0	83.71	42.4

The spectra are fitted using the equivalent circuit model, which is illustrated in Fig. 3b. The detailed resistances of the two electrolytes are summarized in Table 1 [26]. Results indicate that the impedance of the CEI film ( $R_f$ ) of the cell with 0.1% CT additive electrolyte is always smaller than that without CT additive electrolyte during the 300th cycle. Additionally, the  $R_f$  of the cell with 0.1% CT additive electrolyte remains practically unchanged from the initial to the 300th cycle [27]. Results show that the addition of CT to the electrolyte can reduce the impedance of the battery significantly. This effect results from the formation of a more stable surface layer on the surface of the LNMO cathode, and it may be due to the participation of CT, which cannot only inhibit the severe decomposition of the electrolyte but also reduce the dissolution of Mn and Ni during the cycle [28].

To compare the self-discharge difference between the two electrolytes, the self-discharge test was performed by storing the fully charged Li/LNMO battery at room temperature for 4 days. Figure 4 displays the voltage variations during storage of the cells employing electrolytes with and without CT. The voltage of the charged cell employing additive-free electrolyte drops from 4.7 to 3.1 V, while the voltage of the charged cell-employed electrolyte with 0.1% CT additive remains practically unchanged. Results confirm that CT can suppress the decomposition of the electrolyte significantly.

To understand further the effect of CT on the phase stability electrochemical tests of the Li/Li symmetrical cell are conducted and the results are shown in Fig. 5. The electrolyte with 0.1% CT additive has better stability and lower polarization than those of the electrolyte without CT. Specifically,

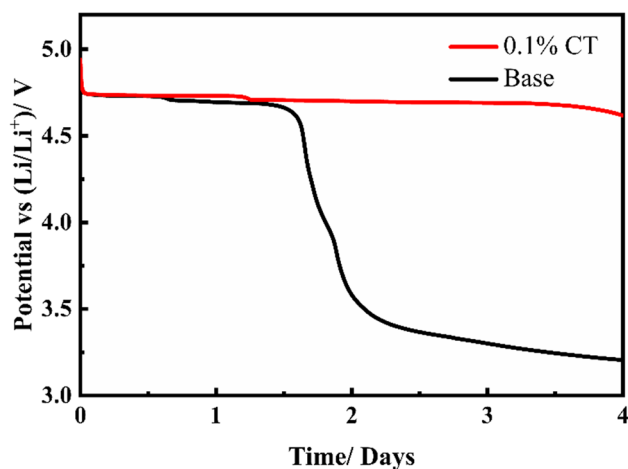


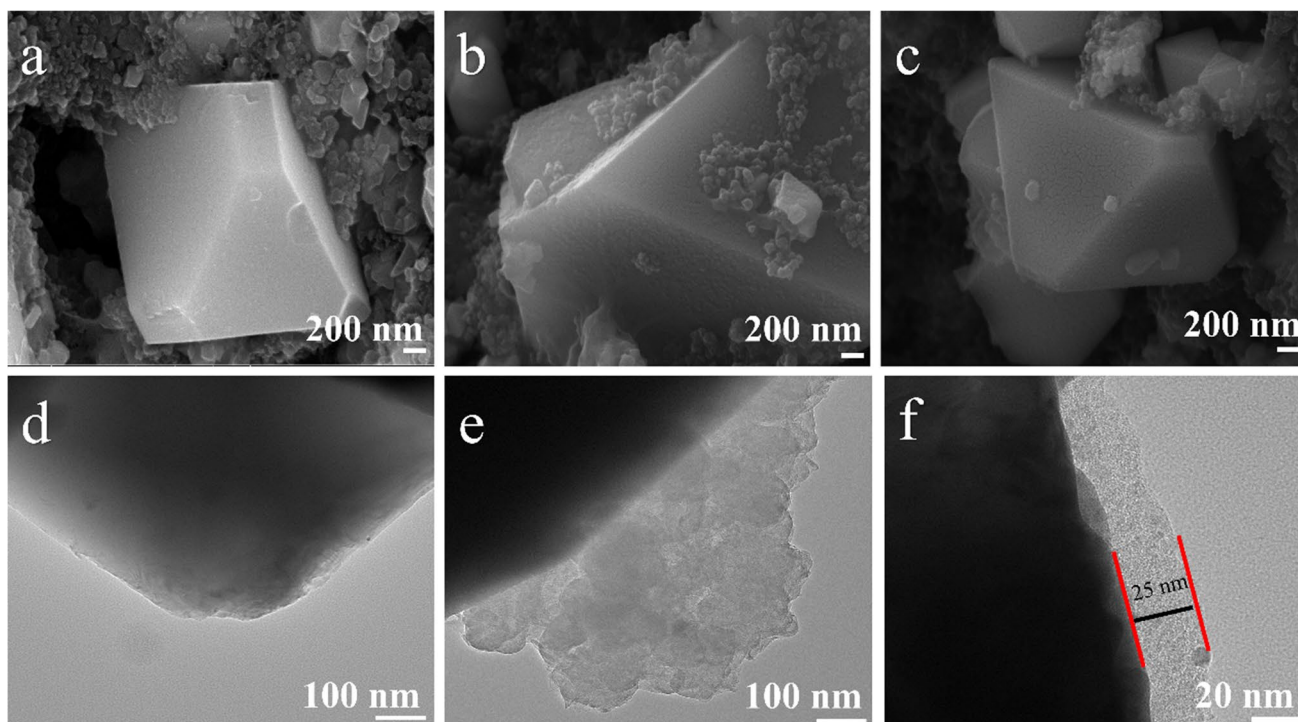
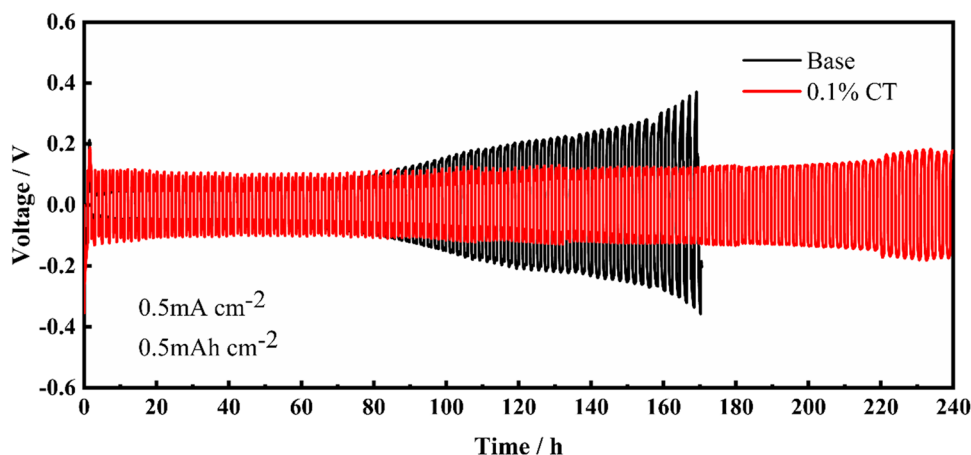
**Fig. 4** Self-discharge curves of Li/LNMO charged cells stored in the electrolyte with and without additive of CT

the polarization and fluctuation of the Li/Li symmetrical cell with the base electrolyte appear after deposition/stripping for approximately 160 h. This is caused by the generation of dendrite Li, leading to an internal short circuit. However, symmetric cells with 0.1% CT additive shows only slight potential polarization even after 240 h of cycling, which is ascribed to the protection of CT for Li metal [29–31].

### Surface morphology and composition characterization

The SEM and TEM images of the fresh and cycled LNMO electrodes are displayed in Fig. 6. Clean and smooth surfaces can be seen on the fresh LNMO particles (Fig. 6a, d). After 300 cycles, the particles in the base electrolyte (Fig. 6b, e) were covered by uneven and thick (100 nm) electrolyte decomposition products, which increased electrode polarization and  $R_f$  of the LNMO cathode. However, the morphology of LNMO of the 0.1% CT additive (Fig. 6c, f) remained smooth with only a uniform thin layer of approximately 25 nm covering the surface of LNMO.

**Fig. 5** Voltage–time profiles of Li||Li symmetric cells using the with and without 0.1% CT additive at the current density of  $0.5 \text{ mA cm}^{-2}$  with a capacity of  $0.5 \text{ mAh cm}^{-2}$ .



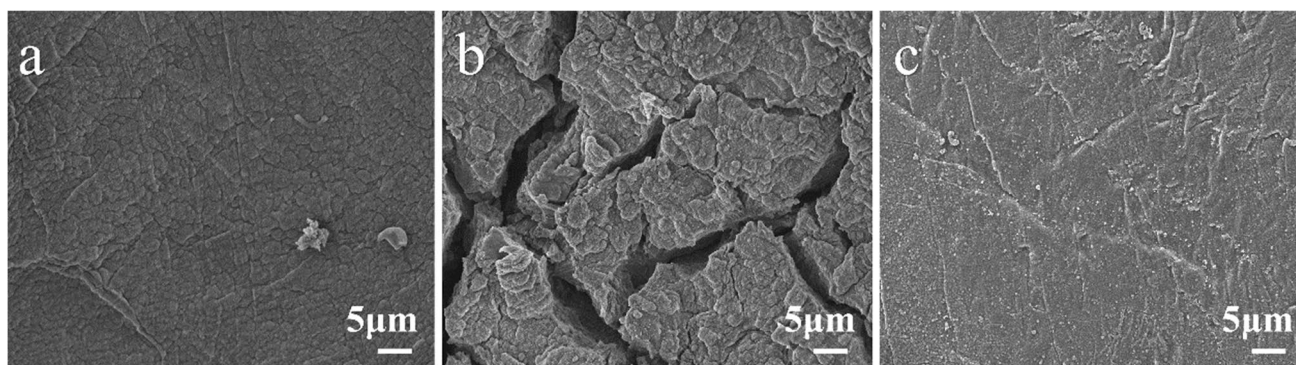
**Fig. 6** SEM and TEM images of the LNMO cathode: fresh (a)(d), after 300 cycles in the electrolyte without (b) (e) and with (c) (f) 0.1% CT additive

Figure 7 shows the SEM images of the lithium anode in the electrolyte with and without 0.1% CT additive. The surface morphology of fresh lithium anode is smooth and clean (Fig. 7a). However, for the anode after 300 cycles in the base electrolyte, the surface of the lithium anode cracks (Fig. 7b). In contrast, the lithium anode cycled in CT-containing electrolyte is flat, uniform, and dense (Fig. 7c). The results indicate that CT additive is favorable to the uniform deposition of lithium ions, and it can suppress the growth of lithium dendrite and can improve the interface stability of lithium anode.

The XRDs of LNMO electrodes before and after 300 cycles are shown in Fig. 8. All electrodes show typical

LNMO spinel diffraction peaks. Compared with the sample before cycling, the peak positions and intensities of the electrode cycled in the electrolyte without CT additive have changed, in which the peak positions shift toward higher angles and peak intensities become weaker. However, the sample after cycling in the electrolyte with 0.1% CT maintained a similar diffraction pattern to the fresh electrode samples.

Results demonstrate that the structure of LNMO particles suffers destruction when cycling in the electrolyte without additive of CT, while maintaining their structural stability when cycling in the electrolyte with an additive of CT [32, 33].



**Fig. 7** SEM images of the Li anode: fresh (a), after 300 cycles in the electrolyte without (b) and with (c) 0.1% CT additive

**Fig. 8** XRD (a) and enlarge (b) patterns of LNMO: fresh and after 300 cycles LNMO electrode samples

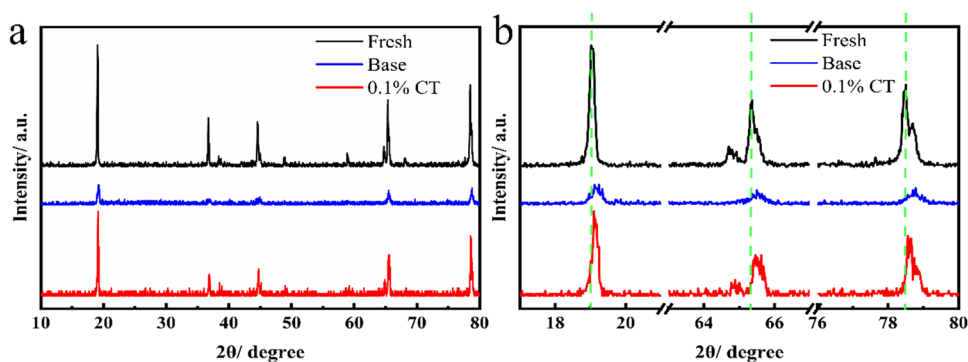
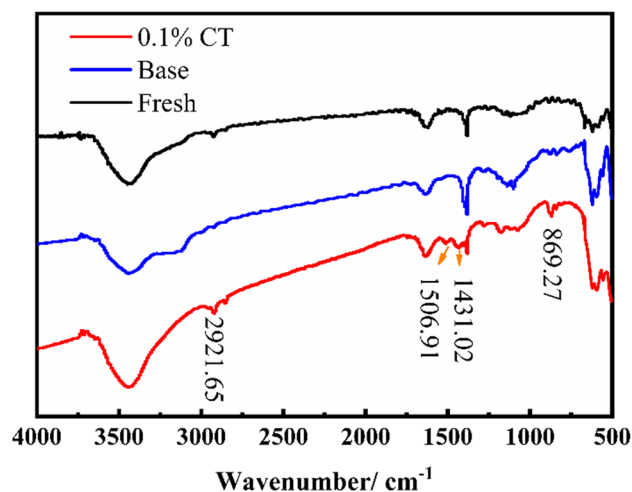


Figure 9 presents the FTIR spectra of LNMO electrodes before and after 300 cycles in the electrolyte with and without additive of CT. Additionally, the LNMO electrode cycled in the electrolyte with an additive of 0.1% CT shows the aromatic ring vibration of polythiophene at 2921.65, 1506.91, and 1431.02  $\text{cm}^{-1}$ . The peak at 869.27  $\text{cm}^{-1}$  is the characteristic of the C-S species [34]. Results show that the oxidation products of CT were deposited on the LNMO cathode surface film.

Furthermore, Li metal was taken from Li/LNMO cells after 300 cycles and dissolved in 3%  $\text{HNO}_3$ . The ICP results of Mn and Ni content on the Li anode in the electrolyte with and without additive of CT are shown in Fig. 10. The contents of Mn and Ni in the electrolyte without additive of CT are 2.205 and 0.732 ppm, respectively. While the values for the electrolyte with additive of 0.1% CT are 0.511 and 0.172 ppm. This suggests that the addition of CT cannot only efficiently prevents the decomposition of the electrolyte but also suppresses the dissolution of transition metal ions from LNMO.

The interphase chemical composition of LNMO electrodes was investigated by XPS (Fig. 11). The fresh LNMO electrode shows three prominent peaks in the C1s spectrum: C–C (284.8 eV) in acetylene black, C–F (289.7 eV), and C–H (286.3 eV) in PVDF binder. In the O1s spectrum, the peak



**Fig. 9** FTIR spectra of LNMO: fresh and after 300 cycles LNMO electrode samples

(530.05 eV) is assigned to the Me–O of LNMO and the peak (531.4 eV) belongs to the  $\text{Li}_2\text{CO}_3$  of C=O [35–37]. In the F 1s spectrum, the peak value (688.1 eV) is attributed to C–F in the PVDF binder [4].

After 300 cycles, two new peaks appear, including C–O (287.5 eV) and C=O (288.1 eV) groups. These groups can

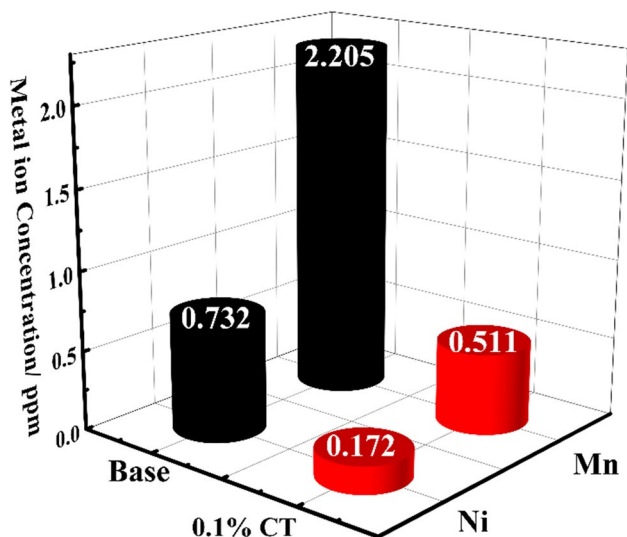


**Fig. 10** Concentrations of Mn and Ni that deposit on the Li electrode after 300 cycles in the electrolyte without and with CT additive

be attributed to  $\text{ROCO}_2\text{Li}$  and  $\text{ROLi}$  species, which result from electrolyte decomposition on the electrode surface. Additionally, after 300 cycles, a novel C-S peak (287.1 eV) appears for the LNMO electrode in the electrolyte with additive of CT, which confirms the formation of polythiophene compounds. After cycling, the LiF and PVDF peak of the LNMO electrode with additive of 0.1% CT electrolyte is weaker than that without additive of CT electrolyte. LiF is an electronic insulator, and a small amount of LiF can improve the stability of the surface film. However, excessive LiF will lead to a significant increase in impedance, affecting the embedding and stripping of  $\text{Li}^+$ .

### Conclusions

The introduction of CT as a bifunctional electrolyte additive into Li/LNMO battery can construct stable SEI and CEI films on the Li anode and LNMO high-voltage cathode surface during the initial charging process. The SEM and TEM images showed that CT could facilitate the formation of a thin and uniform cathode electrolyte interphase film on the electrode surface. Furthermore, XRD and XPS measurements revealed that the CT-formed protection layer can enhance the stability of the interphase effectively, prevent further decomposition of the electrolytes and the dissolution of transition metals, and improve the cycling performance significantly. When a small amount of CT (0.1 wt%) is added to the electrolyte, the capacity retention of Li/LNMO battery increases from 44.18 to 91.2% after 300 cycles. This work demonstrates the considerable potential of CT as a functional additive in high-voltage Li-ion batteries.

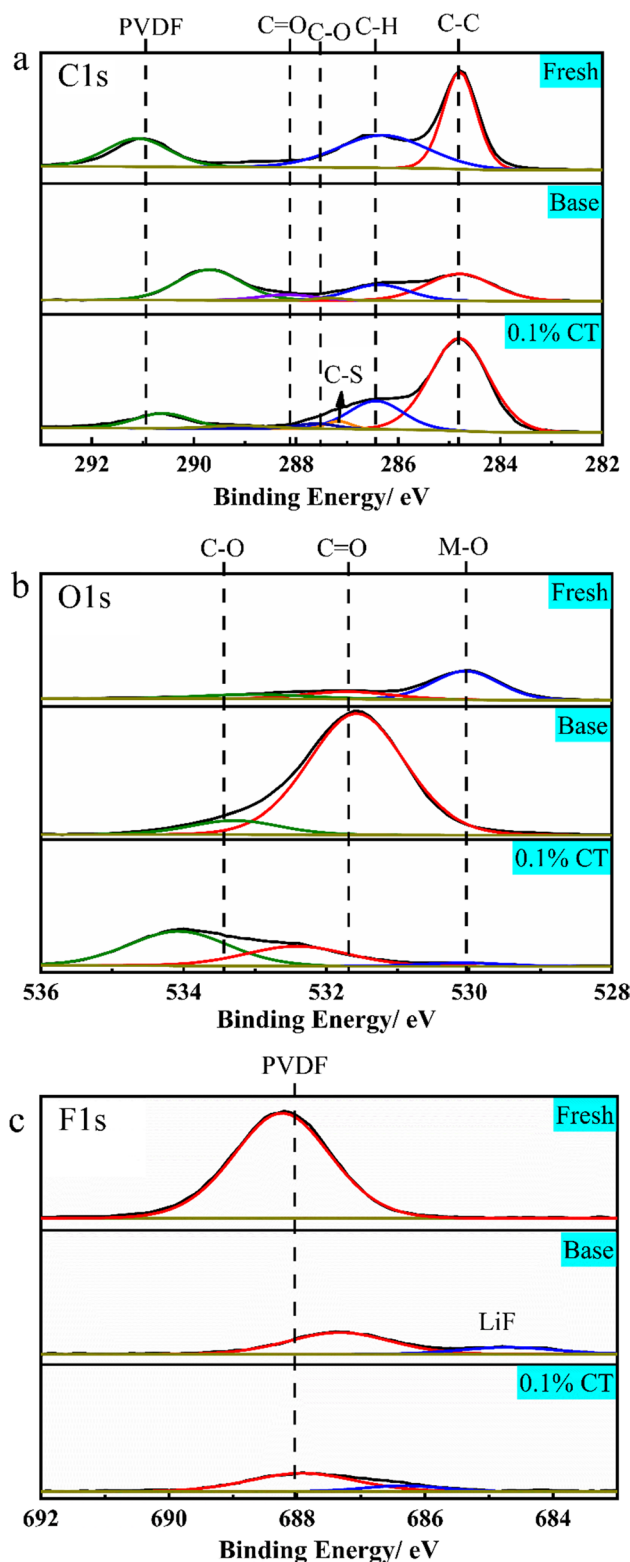


**Fig. 11** XPS patterns of fresh and after 300 cycles LNMO in the electrolyte with and without 0.1% CT additive: C1s (a), O1s (b), and F 1 (c)

**Funding** This work was supported by the National Natural Science Foundation of China.

## Declarations

**Conflict of interest** The authors declare no competing interests.

## References

- Hubble D, Brown DE, Zhao YZ, Fang C, Lau J, McCloskey BD, Liu G (2022) Liquid electrolyte development for low-temperature lithium-ion batteries. *Energy Environ Sci* 15:550–578. <https://doi.org/10.1039/D1EE01789F>
- Liu DD, Xiong XH, Liang QW, Wu XW, Fu HK (2021) An inorganic-rich SEI induced by LiNO<sub>3</sub> additive for a stable lithium metal anode in carbonate electrolyte. *Chem Commun* 57:9232–9235. <https://doi.org/10.1039/D1CC03676A>
- Fan XL, Wang CS (2021) High-voltage liquid electrolytes for Li batteries: progress and perspectives. *Chem Soc Rev* 50:10486–10566. <https://doi.org/10.1039/D1CS00450F>
- Tan CL, Cui LS, Li Y, Qin XJ, Li Y, Pan QC, Zheng FH, Wang HQ, Li QY (2021) Stabilized cathode interphase for enhancing electrochemical performance of LiNi<sub>0.5</sub>Mn<sub>1.5</sub>O<sub>4</sub>-based lithium-ion battery via cis-1,2,3,6-tetrahydrophthalic anhydride. *ACS Appl Mater Interfaces* 13:18314–18323. <https://doi.org/10.1021/acsami.1c01979>
- Wu XM, Chen S, Mai FR, Zhao JH, Li CA, Liu W (2013) Effect of crystallization route on the properties of LiMn<sub>2</sub>O<sub>4</sub> thin films prepared by spin coating. *J Solid State Electrochem* 17:707–711. <https://doi.org/10.1007/s10008-012-1920-3>
- Xiang YH, Jiang YL, Liu SQ, Wu JH, Liu ZX, Zhu L, Xiong LZ, He ZQ, Wu XW (2020) Improved electrochemical performance of 0.5Li<sub>2</sub>MnO<sub>3</sub>·0.5LiNi<sub>0.5</sub>Mn<sub>0.5</sub>O<sub>2</sub> cathode materials for lithium ion batteries synthesized by ionic-liquid-assisted hydrothermal method. *Front Chem* 8:729. <https://doi.org/10.3389/fchem.2020.00729>
- Zhong MM, Guan JD, Feng QJ, Wu XW, Xiao ZB, Zhang W, Tong S, Zhou N, Gong DX (2018) Accelerated polysulfide redox kinetics revealed by ternary sandwich-type S@Co/N-doped carbon nanosheet for high-performance lithium-sulfur batteries. *Carbon* 128:86–96. <https://doi.org/10.1016/j.carbon.2017.11.084>
- Wu XT, Yin CS, Zhang MF, Xie YQ, Hu JJ, Long RL, Wu XM, Wu XW (2023) The intercalation cathode of MOFs-driven vanadium-based composite embedded in N-doped carbon for aqueous zinc ion batteries. *Chem Eng J* 452:139. <https://doi.org/10.1016/j.cej.2022.139573>
- Madinabeitia I, Rikarte J, Baraldi G, Fernández-Carretero FJ, Garbayo I, García-Luis A, Muñoz-Márquez MÁ (2022) Growth parameters and diffusion barriers for functional high-voltage thin-film batteries based on spinel LiNi<sub>0.5</sub>Mn<sub>1.5</sub>O<sub>4</sub> cathodes. *ACS Appl Mater Interfaces* 14:2720–2730. <https://doi.org/10.1021/acsami.1c18247>
- Tian T, Lu L-L, Yin Y-C, Tan Y-H, Zhang T-W, Li F, Yao H-B (2022) Trace doping of multiple elements enables stable cycling of high areal capacity LiNi<sub>0.5</sub>Mn<sub>1.5</sub>O<sub>4</sub> cathode. *Small* 18:2106898. <https://doi.org/10.1002/smll.202106898>
- Bi K, Zhao SX, Huang C, Nan CW (2018) Improving low-temperature performance of spinel LiNi<sub>0.5</sub>Mn<sub>1.5</sub>O<sub>4</sub> electrode and LiNi<sub>0.5</sub>Mn<sub>1.5</sub>O<sub>4</sub>/Li<sub>4</sub>Ti<sub>5</sub>O<sub>12</sub> full-cell by coating solid-state electrolyte Li-Al-Ti-P-O. *J Power Sources* 389:240–248. <https://doi.org/10.1016/j.jpowsour.2018.03.071>
- Feng YH, Xu H, Zhang Y, Li CL, Zhao DN, Zhao QP, Mao LP, Zhang HM, Li SY (2019) Effects of LiBF<sub>4</sub> concentration in carbonate-based electrolyte on the stability of high-voltage LiNi<sub>0.5</sub>Mn<sub>1.5</sub>O<sub>4</sub> cathode. *Ionics* 25:3623–3631. <https://doi.org/10.1007/s11581-019-02960-3>
- Qiu YJ, Lu DS, Gai YY, Cai YP (2022) Adiponitrile (ADN): a stabilizer for the LiNi<sub>0.8</sub>Co<sub>0.1</sub>Mn<sub>0.1</sub>O<sub>2</sub> (NCM811) electrode/electrolyte interface of a graphite/NCM811 Li-ion cell. *ACS Appl Mater Interfaces* 14:11398–11407. <https://doi.org/10.1021/acsami.1c23335>
- Lee KS, Sun YK, Noh J, Song KS, Kim DW (2009) Improvement of high voltage cycling performance and thermal stability of lithium-ion cells by use of a thiophene additive. *Electrochem Commun* 11:1900–1903. <https://doi.org/10.1016/j.elecom.2009.08.012>
- Xia L, Xia YG, Liu ZP (2015) Thiophene derivatives as novel functional additives for high-voltage LiCoO<sub>2</sub> operations in lithium ion batteries. *Electrochim Acta* 151:429–436. <https://doi.org/10.1016/j.electacta.2014.11.062>
- Tu WQ, Xia P, Li JH, Zeng LZ, Xu MQ, Xing LD, Zhang LQ, Yu L, Fan WZ, Li WS (2016) Terthiophene as electrolyte additive for stabilizing lithium nickel manganese oxide cathode for high energy density lithium-ion batteries. *Electrochim Acta* 208:251–259. <https://doi.org/10.1016/j.electacta.2016.05.029>
- Han SY, Liu Y, Zhang H, Fan CJ, Fan WZ, Yu L, Du XY (2020) Succinonitrile as a high-voltage additive in the electrolyte of LiNi<sub>0.5</sub>Co<sub>0.2</sub>Mn<sub>0.3</sub>O<sub>2</sub>/graphite full batteries. *Surf Interface Anal* 52:364–373. <https://doi.org/10.1002/sia.6744>
- Wang XS, Zheng XW, Liao YH, Huang QM, Xing LD, Xu MQ, Li WS (2017) Maintaining structural integrity of 4.5 V lithium cobalt oxide cathode with fumaronitrile as a novel electrolyte additive. *J Power Sources* 338:108–116. <https://doi.org/10.1016/j.jpowsour.2016.10.103>
- Wang L, Ma YL, Li Q, Zhou ZX, Cheng XQ, Zuo PJ, Du CY, Gao YZ, Yin GP (2017) 1,3,6-Hexanetricarbonitrile as electrolyte additive for enhancing electrochemical performance of high voltage Li-rich layered oxide cathode. *J Power Sources* 361:227–236. <https://doi.org/10.1016/j.jpowsour.2017.06.075>
- Duan BY, Hong B, Li J, Qin ZM, Jiang F, Lai YQ (2018) 1, 3, 5-Pentanetricarbonitrile additive for improving high voltage stability of lithium cobalt oxide cells. *Electrochim Acta* 286:86–91. <https://doi.org/10.1016/j.electacta.2018.08.041>
- Ji YJ, Zhang ZR, Gao M, Li Y, McDonald MJ, Yang Y (2015) Electrochemical behavior of suberonitrile as a high-potential electrolyte additive and Co-solvent for Li[Li<sub>0.2</sub>Mn<sub>0.56</sub>Ni<sub>0.16</sub>Co<sub>0.08</sub>]O<sub>2</sub> cathode material. *J Electrochem Soc* 162:A774–A780. <https://doi.org/10.1149/2.1001504jes>
- Lee SH, Hwang JY, Park SJ, Park GT, Sun YK (2019) Adiponitrile (C<sub>6</sub>H<sub>8</sub>N<sub>2</sub>): a new Bi-functional additive for high-performance Li-metal batteries. *Adv Funct Mater* 29:1902496. <https://doi.org/10.1002/adfm.201902496>
- Chen JW, Vatamanu J, Xing LD, Borodin O, Chen HY, Guan XC, Liu X, Xu K, Li WS (2020) Improving electrochemical stability and low-temperature performance with water/acetonitrile hybrid electrolytes. *Adv Engng Mater* 10:1902654. <https://doi.org/10.1002/aenm.201902654>
- Wang J, Zhao DN, Cong YY, Zhang NS, Wang P, Fu XL, Cui XL (2021) Analyzing the mechanism of functional groups in phosphate additives on the interface of LiNi<sub>0.8</sub>Co<sub>0.15</sub>Al<sub>0.05</sub>O<sub>2</sub> cathode materials. *ACS Appl Mater Interfaces* 13:16939–16951. <https://doi.org/10.1021/acsami.0c21535>
- Wang P, Cui XL, Zhao DN, Yan D, Ding H, Dong H, Wang J, Wu SM, Li SY (2022) Effects of soluble products decomposed from chelato-borate additives on formation of solid electrolyte interface layers. *J Power Sources* 535:231451. <https://doi.org/10.1016/j.jpowsour.2022.231451>
- Wang P, Yan D, Wang CY, Ding H, Dong H, Wang J, Wu SM, Cui XL, Li CL, Zhao DN, Li SY (2022) Study of the formation and



- evolution of solid electrolyte interface via in-situ electrochemical impedance spectroscopy. *Appl Surf Sci* 596:153572. <https://doi.org/10.1016/j.apsusc.2022.153572>
27. Wang J, Dong H, Wang P, Fu XL, Zhang NS, Zhao DN, Li SY, Cui XL (2022) Adjusting the solvation structure with tris(trimethylsilyl)borate additive to improve the performance of LNCM half cells. *J Energy Chem* 67:55–64. <https://doi.org/10.1016/j.jechem.2021.09.022>
  28. Zhang DF, Liu M, Ma JB, Yang K, Chen Z, Li KK, Zhang C, Wei YP, Zhou M, Wang P, He YB, Lv W, Yang QH, Kang FY, He YB (2022) Lithium hexamethyldisilazide as electrolyte additive for efficient cycling of high-voltage non-aqueous lithium metal batteries. *Nat Commun* 13:6966. <https://doi.org/10.1038/s41467-022-34717-4>
  29. Chen C, Liang QW, Chen ZX, Zhu WY, Wang ZJ, Li Y, Wu XW, Xiong XH (2021) Phenoxy radical-induced formation of dual-layered protection film for high-rate and dendrite-free lithium-metal anodes. *Angew Chem Int Ed* 60:26718–26724. <https://doi.org/10.1002/anie.202110441>
  30. Zhang QK, Wang K, Wang XS, Zhong YT, Liu MZ, Liu X, Xu K, Fan WZ, Yu L, Li WS (2019) Lithium bis(oxalate)borate reinforces the interphase on Li-metal anodes. *ACS Appl Mater Interfaces* 11:20854–20863. <https://doi.org/10.1021/acsami.9b04898>
  31. Jiang S, Xu X, Yin JY, Wu HH, Zhu XQ, Gao YF (2022) Multifunctional electrolyte additive for Bi-electrode interphase regulation and electrolyte stabilization in Li/LiNi<sub>0.8</sub>Co<sub>0.1</sub>Mn<sub>0.1</sub>O<sub>2</sub> batteries. *ACS Appl Mater Interfaces* 14:38758–38768. <https://doi.org/10.1021/acsami.2c09285>
  32. Cheng FY, Zhang XY, Wei P, Sun SX, Xu Y, Li Q, Fang C, Han JT, Huang YH (2022) Tailoring electrolyte enables high-voltage Ni-rich NCM cathode against aggressive cathode chemistries for Li-ion batteries. *Sci Bull* 67:2225–2234. <https://doi.org/10.1016/j.scib.2022.10.007>
  33. Jiang B, Li JR, Luo B, Yan QZ, Li H, Liu LH, Chu LH, Li YF, Zhang QB, Li MC (2021) LiPO<sub>2</sub>F<sub>2</sub> electrolyte additive for high-performance Li-rich cathode material. *J Energy Chem* 60:564–571. <https://doi.org/10.1016/j.jechem.2021.01.024>
  34. Zhu YM, Luo XY, Zhi HZ, Liao YH, Xing LD, Xu MQ, Liu X, Xu K, Li WS (2018) Diethyl(thiophen-2-ylmethyl)phosphonate: a novel multifunctional electrolyte additive for high voltage batteries. *J Mater Chem A* 6:10990–11004. <https://doi.org/10.1039/C8TA01236A>
  35. Chen HY, Chen JW, Zhang WG, Xie QM, Che YX, Wang HR, Xing LD, Xu K, Li WS (2020) Enhanced cycling stability of high-voltage lithium metal batteries with a trifunctional electrolyte additive. *J Mater Chem A* 8:22054–22064. <https://doi.org/10.1039/D0TA07438A>
  36. Shang HM, Zhou HX, Gao JJ, Zhang H, Li TH, Qiao YJ, Niu WC, Qu MZ, Xie ZW, Peng GC (2021) Improving the cyclic stability of LiNi<sub>0.5</sub>Mn<sub>1.5</sub>O<sub>4</sub> cathode by modifying the interface film with 8-hydroxyquinoline. *ChemistrySelect* 6:3988–3994. <https://doi.org/10.1002/slct.202100754>
  37. Liu FY, Zhang Z, Yu ZY, Fan XM, Yi MY, Bai MH, Song Y, Mao QY, Hong B, Zhang ZA, Lai YQ (2022) Bifunctional nitrileborate based electrolyte additive enables excellent electrochemical stability of lithium metal batteries with single-crystal Ni-rich cathode at 4.7 V. *Chem Eng J* 434:134745. <https://doi.org/10.1016/j.cej.2022.134745>

**Publisher's note** Springer Nature remains neutral with regard to jurisdictional claims in published maps and institutional affiliations.

Springer Nature or its licensor (e.g. a society or other partner) holds exclusive rights to this article under a publishing agreement with the author(s) or other rightsholder(s); author self-archiving of the accepted manuscript version of this article is solely governed by the terms of such publishing agreement and applicable law.